Single-electron states and conductance in lateral-surface superlattices

Marcos H. Degani* and J. P. Leburton
Beckman Institute for Advanced Science and Technology, University of Illinois, Urbana, Illinois 61801
and Coordinated Science Laboratory, University of Illinois, Urbana, Illinois 61801
(Received 26 June 1991)

The electronic properties of a two-dimensional lateral-surface superlattice are simulated by using the split-operator technique based on the solution of the time-dependent Schrödinger equation involving the propagation of the wave functions in the imaginary time domain. The two-dimensional dispersion relation and the density of states are derived and the transport characteristics of the system are calculated in linear-response theory. The results compare well with recent experimental data and show clear evidence of single-electron states in the system.

Recently the problem of a two-dimensional (2D) electron gas in a periodic surface potential has been the subject of many experimental investigations.[1–8] With the advent in nanolithography techniques, periodic structures with nanometer feature sizes can be fabricated in which the wave nature of the electrons is manifested in interference and diffraction effects. As a variation of the ordinary single-gate modulation-doped field-effect transistor, a lateral-surface superlattice (LSSL) is realized by using a grid gate.[2,5] In this system the degree of confinement can be controlled by changing the gate voltage. At sufficiently high negative gate bias, when the gated regions are completely depleted, the ungated regions can retain electrons and the system behaves as an array of isolated quantum dots. When the gate voltage has intermediate values such that the gated regions are not completely depleted the system is a quantum dots superlattice with states extending over several periods of the structure. In the present paper we will focus our attention on the low-energy states bound in the periodic potential and calculate the conductance of weakly periodic LSSL with a simple linear model.

Kumar, Laux, and Stern[9] have studied theoretically the electronic states in a single isolated GaAs quantum dot resulting from a grid gate structure by solving self-consistently the Poisson and Schrödinger equations in three dimensions. They concluded that the effective confining potential has nearly circular symmetry despite the square geometry of the gate and that the energy levels are quite insensitive to the charge in the quantum dot at a fixed gate voltage. For a fixed gate voltage the effective potential has a flat central region and increases rapidly as a function of the distance. In the present paper we capitalize on the results of Kumar, Laux, and Stern[9] to investigate the nature of the discrete electron states in a weakly periodic potential. We take a simple approach by assuming complete confinement in the plane of the electron gas. This is justified since the confinement in the vertical z direction is much stronger than the in-plane confinement. We propose a phenomenological periodic potential[10] which is given by

$$V(x,y)=-V_0\sum_{n,m}\exp\left\{-\left[\left[\frac{x-nl_x}{a}\right]^4+\left[\frac{y-ml_y}{a}\right]^4\right]\right\}, \quad (1)$$

in order to obtain the two-dimensional (2D) dispersion relation, the density of states, the conductance, and the mobility as a function of the Fermi energy for several temperatures. In Eq. (1), V_0 and a are the amplitude and the extension of the potential, respectively. l_x and l_y are the periodicity on the x and y directions, respectively. Figure 1 shows the effective potential used in this simulation with $a=520$ Å. In agreement with the self-consistent results,[9] this model presents a central flat region and increases rapidly as a function of the distance.

The method we have developed to calculate the electronic structure of a two-dimensional periodic system is based on the solution of the time-dependent Schrödinger equation and uses the split-operator technique. For numerical purposes the time-dependent Schrödinger equation is written as[12,13]

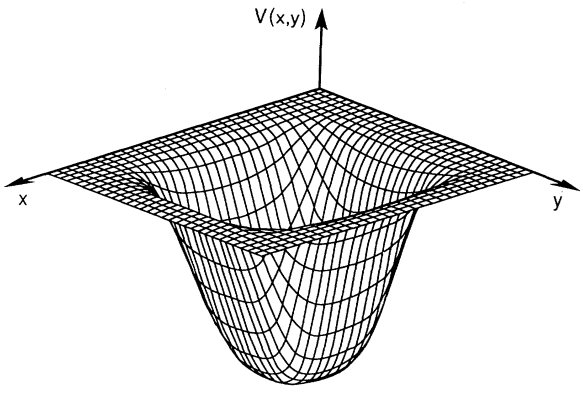

FIG. 1. Effective potential $V(x,y)$ for an $l_x=l_y=200$-nm grid gate with a 60-nm nominal linewidth.

$$\psi(\mathbf{r},t+\Delta t)\cong \exp\left[-\frac{iV(\mathbf{r})\Delta t}{2\hbar}\right]\exp\left[-\frac{i\mathbf{p}^2\Delta t}{2m^*\hbar}\right] \times\exp\left[-\frac{iV(\mathbf{r})\Delta t}{2\hbar}\right]\psi(\mathbf{r},t)+O((\Delta t)^3)\ . \tag{2}$$

The error introduced in this expression is due to the noncommutativity of the kinetic and potential operators and since in Eq. (2) each operator is unitary, the norm is strictly conserved.

The effective potential $V(\mathbf{r})$ and the initial wave function $\psi(\mathbf{r},0)$ are computed on a two-dimensional grid and $\psi(\mathbf{r},0)$ is multiplied by $\exp[-iV(\mathbf{r})\Delta t/2\hbar]$ at each grid point. Because the kinetic energy is diagonal in $\mathbf{k}$ space, we use the fast Fourier transform to perform the second operation in Fourier space. The result is then transformed back into real space where it is multiplied by the third operator $\exp[-iV(\mathbf{r})\Delta t/2\hbar]$ to obtain the wave function at time $t+\Delta t$. This procedure is applied iteratively to calculate the time evolution of the initial wave function.

By using this propagation scheme in the imaginary time domain ($t=-i\tau$) we are able to calculate the eigenstates of the Hamiltonian. We choose a Gaussian wave packet as an initial wave function and reach the ground state of the system after several imaginary-time steps of propagation. The excited states are obtained by the same procedure with the well-known Gram-Schmidt method where the new wave function is given by the expression

$$\psi_i^{\text{new}}(\mathbf{r},t)=\psi_i(\mathbf{r},t)-\sum_{j<i}\langle\psi_j\psi_i\rangle\psi_j(\mathbf{r},t)\ , \tag{3}$$

which assures orthonormality between all states at each time step. Here it is important to stress that, unlike the real-time propagation scheme, the wave functions obtained with the imaginary-time propagation must be normalized in each time step.

For periodic systems the wave functions satisfy Bloch's theorem; therefore in order to calculate the dispersion relation we have performed the propagation of a set of wave functions for several subbands and different $\mathbf{k}$ values. This method is numerically quite stable and powerful in providing general solutions for bound states in the confining potential as well as extended high-energy states in the two-dimensional continuum.

The conductance along the x direction is calculated in linear-response theory and is given by

$$G_x=\frac{e^2\tau L_y}{A\hbar^2 L_x}\sum_{\mathbf{k},n}\left[\frac{\partial E_n(\mathbf{k})}{\partial k_x}\right]^2\left[-\frac{\partial f}{\partial E_n}\right]\ , \tag{4}$$

where L_x and L_y are the sizes of the system in the x and y directions, respectively, A is the area of the unit cell, and f is the Fermi-Dirac distribution function. In this preliminary analysis we have assumed a relaxation time τ independent of energy because of the narrowness of the energy range ($\approx$4 meV). In Eq. (4), τ is a parameter that is determined empirically by fitting the experimental G value.

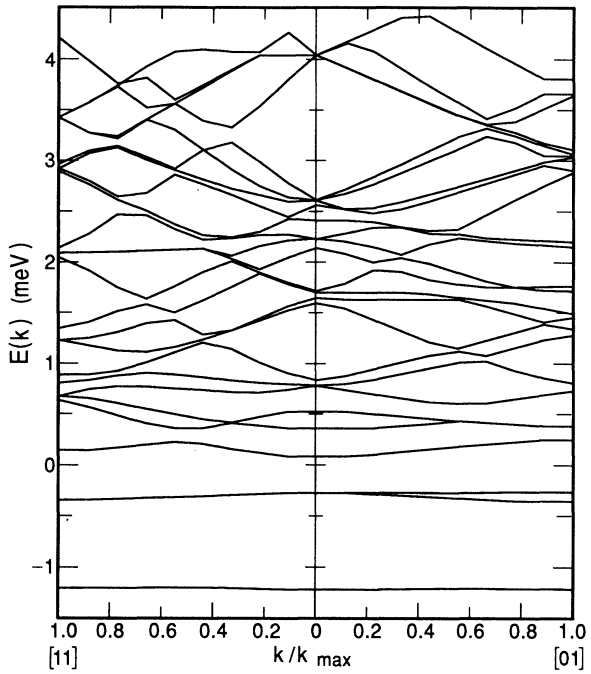

FIG. 2. Dispersion relation for both directions [01] and [11] for the same grid size of Fig. 1 and $V_0=2$ meV.

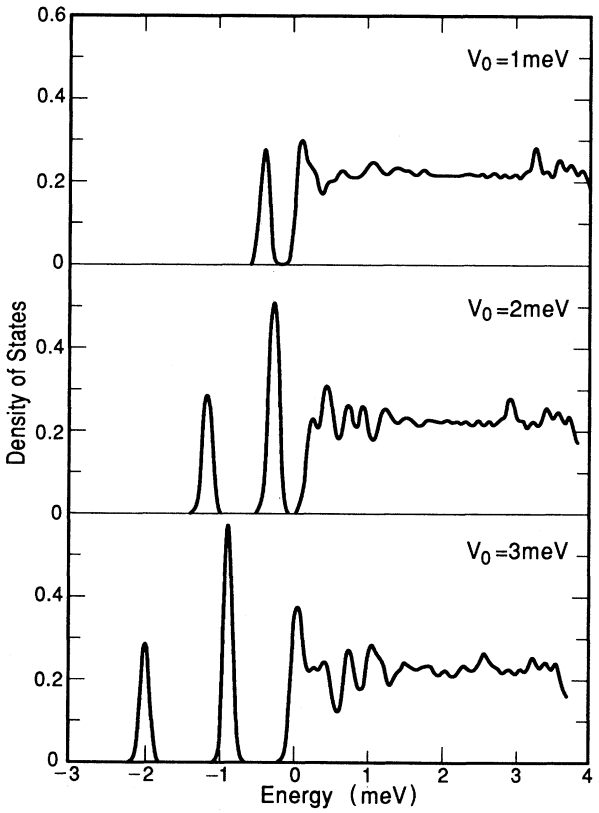

FIG. 3. Density of states (DOS) for the same grid size of Fig. 1 and potential amplitude $V_0=1$, 2, and 3 meV. We have normalized the DOS in order to facilitate a comparison between three V_0 values. The zero of energy is defined at the top of the potential.

We focus our investigation on weakly confining potential with barrier height of few meV which corresponds to the experimental situation of Toriumi *et al.*,[11] who use an $l_x = l_y = 200$-nm square grid gate with nominal width 60 nm. We have carried out the calculation for three different potential amplitudes: 1, 2, and 3 meV and restricted the simulation to the 25 lowest subbands. In Fig. 2 the 2D dispersion relation is plotted against the wave vector in both directions [01] and [11] for a potential amplitude $V_0 = 2$ meV. The zero of energy is defined at the top of the potential. This system presents a very complicated energy subbands dispersion with strong interaction between subbands. The lowest three subbands are relatively flat, which manifest the nature of bound states in the wells. Due to the potential symmetry the second and third subbands are degenerated for almost all values of **k**. For higher energies, the extended states have a complicated dispersion relation which is due to the band folding in the Brillouin zone. Overall the electron effective mass is substantially larger than the bulk effective mass; as a consequence of this, an enormous reduction of the mobility is expected. The density of states is presented in Fig. 3 for three different values of the potential by using an energy broadening of 1.5 K. It can be seen that for $V_0 = 2$ and 3 meV, the two peaks with negative energy correspond to bound states. In fact, the second peak corresponds to the second and third subbands which are almost degenerated for all values of **k**; those states are occupied by four electrons. For the case where the potential amplitude is 1 meV only one bound state exists. In the continuum, the density of states presents several peaks reflecting the influence of quasilocalized states in the periodic potential, and a flat region characteristic of the quasi-two-dimensional nature of the system appears at high energy. In Fig. 4 we show the number of electrons as a function of the Fermi energy for two different temperatures, the low-energy plateaus represent discrete energy states occupied by single electrons. As expected, the transition between plateaus smoothens with temperature; at higher energies the number of electrons is a linear

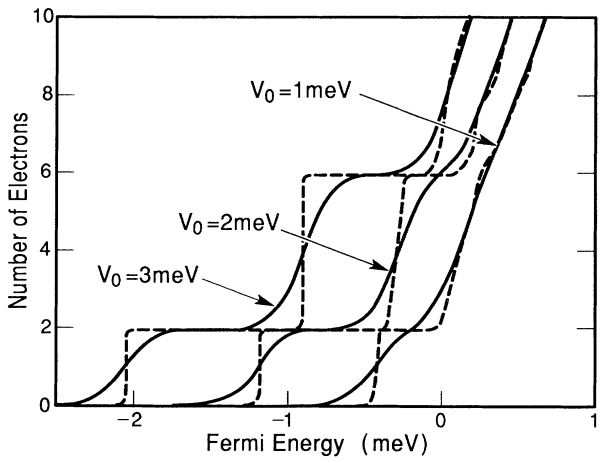

FIG. 4. Number of electrons as a function of the Fermi energy for a potential amplitude $V_0 = 1$, 2, and 3 meV, at $T = 1$ K (solid curves) and $T = 0.1$ K (dashed curves).

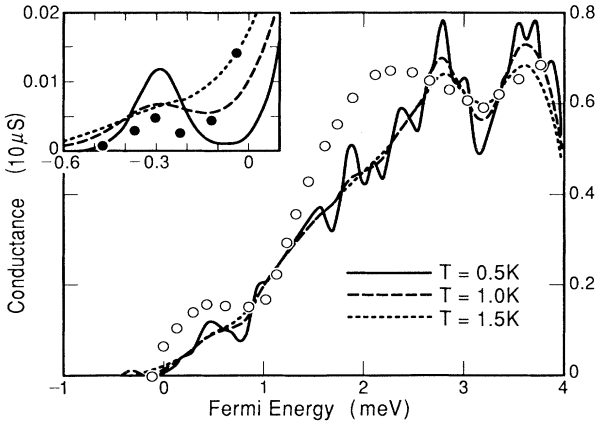

FIG. 5. Conductance as a function of the Fermi energy for $T = 0.5$, 1.0, and 1.5 K. Open circles are experimental data from Ref. 6. The inset shows the first peak of the conductance, dots are experimental results.

function of the Fermi energy. The conductance along the x direction is presented in Fig. 5 as a function of the Fermi energy with the experimental results obtained at 1.5 K. The good agreement obtained with the value of $\tau = 0.35$ ps fitted from the experimental data is especially visible around the valley at $E = 3$ meV. However, our results are strongly dependent on the temperature and for $T = 1.5$ K the fine structures are no longer observable. This is particularly noticeable with the first peak of the conductance which is due to the quasibound energy state at -0.3 meV (inset). It is expected that a more sophisti-

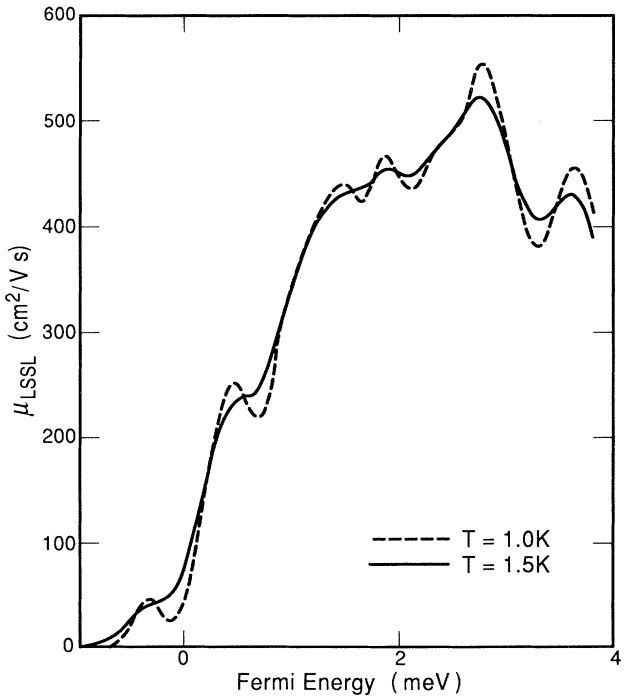

FIG. 6. Electronic mobility for two temperatures $T = 1.0$ K (dashed curves) and $T = 1.5$ K (solid curves).

cated model where the energy dependence of τ is taken into account would reproduce the negative differential features in the conductance at $E=-0.3$ meV. Another important limitation of our model is the assumption of a linear relation between gate bias and Fermi energy in comparing the experimental conductance with the calculated results. Because the localized low-energy states can only accommodate a finite number of electrons, the Fermi energy does not change continuously with the gate voltage, but is rather pinned on the localized state for a finite range of external bias and then jumps from the top of a miniband to the bottom of the next one.[14] This would explain why the experimental curve shows a pronounced and persistent plateau at 0.5 meV where the $E-k$ dispersion is very flat at these energies. Finally, Fig. 6 shows the mobility μ as a function of the Fermi energy for a potential amplitude of 2 meV and for two different temperatures. The important finding here is the substantial reduction of the LSSL mobility compared with the 2D mobility ($\mu_{2D}\approx 3\times 10^5$ cm^2/V s) in uniform gate structures. This μ reduction is due to the presence of the periodic potential modulation which affects considerably the energy dispersion relation.[15]

In conclusion, we have calculated the electronic band structure of a lateral-surface superlattice using a phenomenological potential. The carrier dispersion relation in the LSSL periodic potential is derived to calculate the conductance in the linear-response approximation. The results compare well with recent experimental data and reveal the existence of discrete single-electron states in the system.

One of the authors (M.H.D.) would like to thank the hospitality extended to him during his visit at Beckman Institute. This work was supported by NSF Grant No. EET87-19100.

---

*Permanent address: Instituto de Física e Química de São Carlos, Universidade de São Paulo, Departamento de Física e Ciência dos Materiais, 13560 São Carlos, São Paulo, Brazil.

[1]H. Sakaki, K. Wagatsuma, J. Hamasaki, and S. Saito, Thin Solid Films **36**, 497 (1976).

[2]G. Bernstein and D. K. Ferry, Superlatt. Microstruct. **2**, 373 (1986).

[3]A. C. Warren, D. A. Antoniadis, and H. I. Smith, Phys. Rev. Lett. **56**, 1858 (1986).

[4]T. P. Smith III, H. Arnot, J. M. Hong, C. M. Knoedler, S. E. Laux, and H. Schmid, Phys. Rev. Lett. **59**, 2801 (1987).

[5]K. Ismail, W. Chu, A. Yen, D. A. Antoniadis, and H. Smith, Appl. Phys. Lett. **52**, 1072 (1988); **54**, 460 (1989).

[6]C. T. Liu, D. C. Tsui, M. Shayegan, K. Ismail, D. A. Antoniadis, and H. I. Smith, Solid State Commun. **75**, 395 (1990), and references therein.

[7]C. T. Liu, K. Nakamura, D. C. Tsui, K. Ismail, D. A. Antoniadis, and H. I. Smith, Surf. Sci. **228**, 527 (1990).

[8]P. H. Beton, E. S. Alves, P. C. Main, L. Eaves, M. W. Dellow, M. Henini, O. H. Hughes, S. P. Beaumont, and C. D. W. Wilkinson, Phys. Rev. B **42**, 9229 (1990).

[9]A. Kumar, S. E. Laux, and F. Stern, Phys. Rev. B **42**, 5166 (1990).

[10]We have tested several models for the effective potential. They produce qualitatively the same results, but quantitatively a better result is obtained using the potential defined in Eq. (1).

[11]A. Toriumi, K. Ismail, M. Burkhardt, D. A. Antoniadis, and H. I. Smith, Phys. Rev. B **41**, 12 346 (1990).

[12]R. Kosloff, J. Phys. Chem. **92**, 2087 (1988).

[13]M. H. Degani, Appl. Phys. Lett. **59**, 57 (1991).

[14]M. H. Degani and J. P. Leburton (unpublished).

[15]Additional scattering is due to fluctuations in the periodic potential.